



Selective oxidation of styrene catalyzed by cerium-doped cobalt ferrite nanocrystals with greatly enhanced catalytic performance



Jinhui Tong^{a,*}, Wenyan Li^a, Lili Bo^b, Huan Wang^b, Yusen Hu^b, Zhixia Zhang^b, Abdulla Mahboob^{c,*}

^a College of Chemistry and Chemical Engineering, Northwest Normal University, Lanzhou 730070, People's Republic of China

^b College of Science, Gansu Agricultural University, Lanzhou 730070, People's Republic of China

^c Department of Chemistry, School of Science and Technology, Nazarbayev University, 53 Kabanbay Batyr Avenue, Astana 010000, Kazakhstan

ARTICLE INFO

Article history:

Received 21 July 2016

Revised 1 October 2016

Accepted 3 October 2016

Keywords:

Sol–gel autocombustion

Magnetic nanocrystals

Rare-earth-doped ferrites

Styrene oxidation

Hydrogen peroxide

ABSTRACT

The rare earth metal Ce-doped cobalt ferrite samples $\text{Ce}_x\text{Co}_{1-x}\text{Fe}_2\text{O}_4$ ($x = 0.1, 0.3, 0.5$) were prepared by the sol–gel autocombustion route. The as-prepared samples were characterized by X-ray diffractometry, scanning electron microscopy, transmission electron microscopy, ICP–atomic emission spectroscopy, and N_2 physisorption. Their catalytic performance was evaluated in oxidation of styrene using hydrogen peroxide (30%) as oxidant. Compared with pristine CoFe_2O_4 , the Ce-doped samples were found to be more efficient catalysts for the oxidation of styrene to benzaldehyde, with greatly enhanced catalytic performance. Especially, when $\text{Ce}_{0.3}\text{Co}_{0.7}\text{Fe}_2\text{O}_4$ was used as catalyst, 90.3% styrene conversion and 91.5% selectivity for benzaldehyde were obtained at 90 °C for 9 h reaction. The catalyst can be magnetically separated easily for reuse, and no obvious loss of activity was observed when it was reused in five consecutive runs.

© 2016 Elsevier Inc. All rights reserved.

1. Introduction

Nanospinel ferrites with the general formula AB_2O_4 , as a class of chemically and thermally stable materials, are of great fundamental and technological importance due to their structural, electronic, magnetic, and catalytic properties [1–4]. The complex metal oxides have been widely used in diverse areas such as magnetic recording and separation [5], ferrofluids [6], magnetic resonance imaging (MRI) [7], biomedicine [8], gas sensors [9], high-quality ceramics [10,11], and superparamagnetic materials [12–14]. Especially, they have been widely used as catalysts in liquid phase reactions due to their redox and magnetic recovery properties [15]. As a matter of fact, these catalysts can be separated from a reaction medium by simply placing a magnetic field on the surface of a flask. Spinel ferrites are found to be highly active toward a number of industrial processes, such as oxidative dehydrogenation of hydrocarbons [16,17], decomposition of hydrogen peroxide [18], treatment of automobile-exhaust gases [19], oxidation of various compounds such as chlorobenzene [20], phenol hydroxylation [21], alkylation reactions [22–24], hydrodesulfurization of crude petroleum [20], and catalytic combustion of methane [25,26].

The physical and chemical properties of the ferrites are strongly dependent on their shapes, sizes, and constituents, which are closely related to the method of preparation [27–29]. A widely adopted strategy for synthesizing new ferrites with various constituents and properties is doping other elements in the pristine ferrites [30–35]. As for preparation methods, a most popular one is the sol–gel autocombustion method. This method combines the advantages of chemical sol–gel and combustion processes and gives rise to a thermally induced anionic redox reaction. The energy released from the reaction between oxidant and reductant is adequate to form a desirable phase within a very short time. The process exhibits the advantages of inexpensive precursors and a simple preparation process and can produce highly reactive nano-sized powder [36,37].

Catalytic oxidation of styrene at side chains is of great interest for both academic research and utilization in the industry, because the products styrene oxide and benzaldehyde are important and versatile synthetic intermediates in chemical industries [38]. Especially, benzaldehyde is a very valuable chemical that has widespread applications in perfumery, pharmaceuticals, dyestuffs, and agrochemicals [39]. Traditionally, this reaction has been carried out in both homogeneous and heterogeneous catalyst systems [40–42]. However, homogeneous catalysts have recently become less attractive because of difficulty in separating products and catalysts. Thus, heterogeneous catalysts have currently been paid much attention [43]. Various kinds of catalysts have been

* Corresponding authors. Fax: +86 931 7971533 (J. Tong).

E-mail address: jinhuitong@126.com (J. Tong).

employed to catalyze styrene oxidation [44]. From the viewpoint of environmental protection, molecular oxygen was used as a green and cheap oxidant, for which MOF-74(Cu/Co) [45], bulk Au particles [46], and gold nanoparticles supported on dendrimer resin [47], sulfur-doped graphene [48], and hollow iron oxide nanoshells [49] have been reported to be active catalysts. However, as a mild oxidant, molecular oxygen is usually less efficient, with a low reaction rate at ambient pressure. Compared with molecular oxygen, H_2O_2 is a green and more efficient alternative. Various catalysts have been used to catalyze styrene oxidation using H_2O_2 as oxidant, such as N_4O_4 -type bis(diazoimine) complexes supported on silica [50], platinum nanoclusters supported on TiO_2 anatase [51], phosphomolybdic acid supported on ionic-liquid-modified MCM-41 [52], zinc phthalocyanine supported on multiwalled carbon nanotubes [53], Ag- WO_3 catalyst [54], V-MCM-48 [55], Ti-containing mesoporous silica [56], and iron oxide nanoparticles supported on mesoporous silica-type materials [57]. Based on the mentioned advantages of ferrites, several examples have been reported for oxidation of styrene using ferrites as catalysts, such as nickel and zinc ferrites [26], SrFe_2O_4 [28], $\text{Mg}_x\text{Fe}_{3-x}\text{O}_4$ [29], CaFe_2O_4 [58], Ni-Gd ferrites [59], spinel Mg-Cu ferrites [60], and supported noble metals [1,54,61]. Being a terminal olefin, styrene is difficult to oxidize, and most of these oxidation reactions were limited by complicated preparation procedures, high costs, harsh conditions, or low efficiency.

In our previous work [62], CoFe_2O_4 nanocrystals synthesized by sol-gel autocombustion were proved to be a highly active and easily recovered catalyst for the oxidation of cyclohexane by molecular oxygen without addition of solvents or reductants. As part of our interest in hydrocarbon oxidation catalyzed by spinel ferrites, we are reporting here that rare earth metal Ce-doped cobalt ferrites synthesized by a sol-gel autocombustion method can efficiently catalyze the oxidation of styrene to produce benzaldehyde, and their catalytic activities can be greatly enhanced when compared with those of pristine CoFe_2O_4 and CeO_2 .

2. Experimental

2.1. Materials and equipment

All reagents were of analytical grade and were used as received. X-ray diffraction (XRD) patterns of the samples were collected using a PANalytical X'Pert Pro diffractometer with $\text{CuK}\alpha$ radiation. Scanning electron microscopy (SEM) and transmission electron microscopy (TEM) micrographs were obtained using a JSM-5600LV and a Hitachi H-600 microscope, respectively. Metal content was determined by inductively coupled plasma (ICP) on a Perkin-Elmer ICP/6500 atomic emission spectrometer. BET surface area measurements were performed on a Micromeritics ASAP 2010 instrument at liquid nitrogen temperature. The oxidation products were determined by an HP 6890/5973 GC/MS instrument and quantified by a Shimadzu GC-2010 gas chromatograph using toluene as internal standard.

2.2. Preparation of the catalysts

The rare earth metal cerium-doped cobalt ferrite samples $\text{Ce}_x\text{Co}_{1-x}\text{Fe}_2\text{O}_4$ ($x = 0.1, 0.3, 0.5$) were prepared by a sol-gel autocombustion route under optimized conditions reported in our previous work [62]. In a typical procedure, stoichiometric amounts of $\text{Co}(\text{NO}_3)_2 \cdot 6\text{H}_2\text{O}$, $\text{Ce}(\text{NO}_3)_3 \cdot 6\text{H}_2\text{O}$, $\text{Fe}(\text{NO}_3)_3 \cdot 9\text{H}_2\text{O}$, and citric acid were completely dissolved in distilled water with a 1:1 molar ratio of metals to citric acid and a 0.1 mol L^{-1} concentration of metals. Concentrated ammonia (25–28%) was added slowly under constant stirring to adjust the solution to neutral. The solution was

evaporated in an oil bath at 80°C under continuous stirring until a brown gel formed. After the reaction, the formed gel was dried at 120°C until a foamy xerogel was obtained. Then the produced xerogel was ignited at 650°C , a self-propagating combustion process occurred, and an olive brown product was obtained after it combusted completely. The Ce-doped samples were prepared as described above and were designated as **CFO-Ce_{0.1}**, **CFO-Ce_{0.3}**, and **CFO-Ce_{0.5}**, respectively. For comparison, pristine CoFe_2O_4 was also prepared and was designated as **CFO-A**. The samples were ground finely and screened by a 300 mesh sieve before characterization and employment as catalysts for oxidation of styrene with hydrogen peroxide.

2.3. Oxidation of styrene

The selective oxidation of styrene was carried out in a 25 mL Schlenk tube. In a typical procedure, 0.06 mmol (ca. 15.0 mg, based on the given formula $\text{Ce}_x\text{Co}_{1-x}\text{Fe}_2\text{O}_4$) of catalyst, 2.0 mL (17.4 mmol) of styrene, 10 mL of solvent, and 2.7 mL of hydrogen peroxide (30%), styrene: H_2O_2 molar ratio of 2:3, were added successively into the flask. The flask was then immersed in an oil bath at a desired temperature for a desired reaction time under stirring with an optimum stirrer speed of 1200 rpm, at which the highest conversion rate could be obtained (Fig. S1; see the Supporting Information). It is clear from Fig. S1 that the reaction is effected by diffusion limitation. Under the above conditions, the atmosphere in the tube included mainly air, vapor of substrate, water, and solvent, and oxygen from decomposition of H_2O_2 . The pressure in the tube ranged from 1.1 to 1.2 atm. After the reaction, the tube was cooled to room temperature. The gas-phase mixture was collected and analyzed by gas chromatography (GC) equipped with a 5A molecular sieve column and a thermal conductivity detector (TCD). Liquid-phase aliquots were identified by GC-MS and quantified by GC equipped with an SE-54 capillary column and a hydrogen flame ionization detector (FID) using toluene as internal standard. The detected products in the liquid phase included the main product benzaldehyde and byproducts phenylacetaldehyde, styrene oxide, benzoic acid, phenylacetic acid, and formaldehyde. Trace of CO was detected in the gas phase. The amount of residual H_2O_2 was determined by iodometric titration [63,64] and the H_2O_2 utilization efficiency was defined as follows: H_2O_2 utilization efficiency = $[(\text{mol (benzaldehyde + phenylacetaldehyde + styrene oxide)} + 2 \times \text{mol (benzoic acid + phenylacetic acid)}) / \text{mol (H}_2\text{O}_2)_{\text{consumed}}] \times 100\%$.

3. Results and discussion

3.1. Characterization of the catalysts

3.1.1. The XRD characterization

The XRD patterns of the Ce-doped samples are shown in Fig. 1. The average particle sizes (based on the Scherrer equation) and lattice parameters (based on the formula $a = d\sqrt{h^2 + k^2 + l^2}$, $2d \sin \theta = n\lambda$) based on the most intense diffraction peaks of the spinel phase of the samples are shown in Table 1. It can be confirmed from Fig. 1 that the main phase in Ce-doped samples is spinel (JCPDS No. 22-1086). It can also be confirmed that the minor new phases of CeO_2 (PDF No. 801792) formed and their contents increased with increasing Ce content.

Table 1 shows that the lattice parameters of the Ce-doped samples increased from 8.3812 to 8.3870 Å with increase of Ce from 0 to 0.5. This confirms that Ce^{4+} , with a larger radius of 0.101 nm, partly replaced Co^{2+} or Fe^{3+} , with small radii of 0.082 and 0.067 nm, respectively.

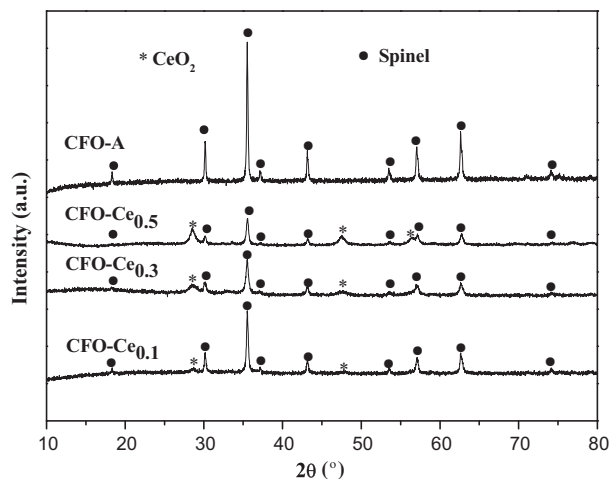


Fig. 1. The XRD patterns of the Ce-doped samples.

Table 1

The XRD average particle sizes, lattice parameters, and BET surface areas of the samples.

Catalyst	XRD average particle size (nm)	Lattice parameter (Å)	BET surface area (m ² g ⁻¹)
CFO-A	24	8.3812	38.6
CFO-Ce _{0.1}	29	8.3824	37.5
CFO-Ce _{0.3}	23	8.3847	38.4
CFO-Ce _{0.5}	21	8.3870	38.9

The mean particle sizes of the samples, based on the Scherrer equation, are 24, 29, 23, and 21 nm for **CFO-A**, **CFO-Ce_{0.1}**, **CFO-Ce_{0.3}**, and **CFO-Ce_{0.5}** respectively.

Metal content of the samples determined by ICP-atomic emission spectroscopy is listed in Table 2. As can be seen, the determined metal contents are consistent with the calculated ones.

3.1.2. The SEM and TEM characterization

The morphologies of the samples were also characterized by SEM and TEM. The SEM and TEM images of the sample **CFO-Ce_{0.3}** are shown in Fig. 2 as representations. The sample **CFO-Ce_{0.3}** features nanoparticles with an irregular morphology and a broad particle size distribution ranging from 10–20 to 30–50 nm, with a large percentage of small particles (25–30 nm). The other samples showed similar morphologies, except for different particle sizes, as calculated from the Scherrer equation based on the XRD patterns.

3.1.3. N₂ physisorption characterization

N₂ physisorption measurements were also performed for the as-prepared samples. The BET surface areas of the samples are summarized in Table 1. It can be seen that the samples showed similar BET surface areas, around 38 m²/g.

3.2. Catalysis tests

The results of styrene oxidation over the as-prepared samples are listed in Table 3. As shown in Table 3, in the absence of catalyst, almost no reaction took place, as seen from GC/MS analysis (entry

Table 2

Metal content of the samples.

Catalyst	Co content (wt.%)	Fe content (wt.%)	Ce content (wt.%)
CFO-A	25.62	46.64	–
CFO-Ce _{0.1}	22.29	45.08	5.66
CFO-Ce _{0.3}	16.25	42.25	15.92
CFO-Ce _{0.5}	10.91	39.76	24.96

1). All the samples can efficiently catalyze the oxidation of styrene, and benzaldehyde was found to be the major product in all cases. As expected, the Ce-doped ferrite samples have shown better performance than pristine CoFe₂O₄ and CeO₂ in enhancement of styrene conversion and benzaldehyde selectivity. Especially in the case of the sample **CFO-Ce_{0.3}**, 59.4% styrene conversion and 88.2% benzaldehyde selectivity were obtained, which is 26.5%, 28.6%, and 22.9%, 41.0% higher than those obtained over pristine CoFe₂O₄ and CeO₂, respectively. The Ce-doped samples also obtained higher H₂O₂ utilization efficiency, except for the sample **CFO-Ce_{0.5}** and CeO₂. It is also clear that the samples have shown much higher activities in both styrene conversion and benzaldehyde selectivity than the reported analogous ferrites [26,65] (entries 7, 8) and supported noble metal catalysts [39] (entry 9).

Increase in catalytic activity can be thought of as linked to the appearance of the CeO₂ face in the XRD. CeO₂ is a known oxidation catalyst. The likely mechanism involves coordination of the organic ligand and the H₂O₂ on Ce³⁺ sites on CeO₂, as previous kinetics studies support this hypothesis [65]. However, it is possible to overload the Ce³⁺ site on CeO₂ with H₂O₂. In addition to the expansion of the lattice due to the introduction of the larger Ce atom in lieu of Fe, the overloading of the Ce³⁺ by H₂O₂ could be a plausible explanation for the optimal performance of the **CFO-Ce_{0.3}** when compared with **CFO-Ce_{0.5}** and CeO₂. We are currently investigating the possibility of cooperative interactions between the Fe atoms and the Ce atoms, as it relates to the optimal performance of the CFO-Ce_{0.3}.

We have performed geometry optimization of a plausible coordination geometry of styrene and H₂O₂ at CeO₂ face using the pseudopotential method implemented in the Siesta package [66]. The coordination geometry (Fig. S2; see the Supporting Information) shows a slight sp³ character on the terminal vinyl carbon, suggesting that coordination onto the Ce³⁺ can activate the terminal vinyl carbon for attack by H₂O₂.

In pursuit of high benzaldehyde selectivity, the sample **CFO-Ce_{0.3}** was chosen as catalyst to optimize the reaction conditions and investigate the recyclable performance of the catalyst.

3.3. Effect of catalyst amount

Table 4 shows the effects of the catalyst amount on the results of styrene oxidation. As can be seen, 5.9 and 9.6% increases in the styrene conversion and benzaldehyde selectivity, respectively, were obtained when the catalyst amount increased from 10.0 to 15.0 mg. However, the selectivity for benzaldehyde decreased to 82.4% when the catalyst amount increased further to 20.0 mg, with only a marginal increase of 2.6% in styrene conversion, possibly due to increasing magnetic agglomeration of the catalyst with increased catalyst amount, which reduced the contact of reactants with the active sites of the catalyst. This is based on the fact that the reaction is affected by diffusion limitation (Fig. S1 in the Supporting Information). The highest H₂O₂ utilization efficiency was obtained when 15.0 mg catalyst was used. Based on these facts, 15.0 mg was selected as the optimum catalyst amount in the following investigations.

3.4. Effect of the solvents

Table 5 shows effects of different solvents on styrene conversion and products distribution over the sample **CFO-Ce_{0.3}**. The order of decrease of dielectric constants for the solvents is H₂O (78.3) > DMF (36.7) > CH₃CN (35.9) > acetylacetone (23.1) > tert-butanol (12.9) > pyridine (12.5) > toluene (2.4) > 1,4-dioxane (2.0). This is also the order of decrease of styrene conversion and the order of increase of benzaldehyde selectivity, except for 1,4-dioxane (entry 5) and water (entry 8). The results have shown that

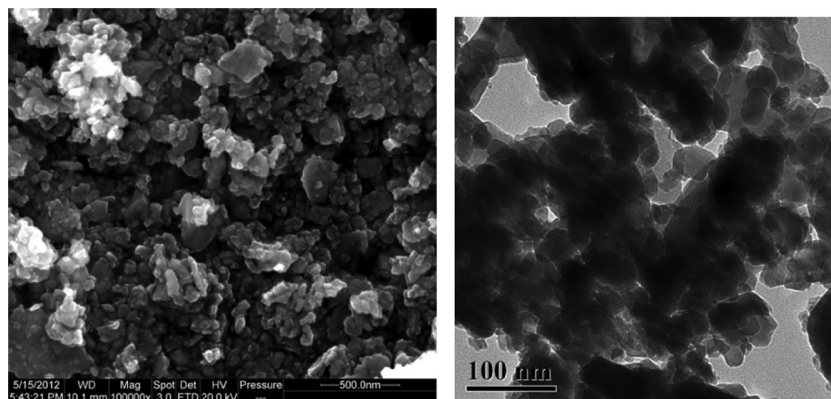


Fig. 2. The SEM and TEM images of the sample **CFO-Ce_{0.3}**.

Table 3

Oxidation of styrene over the as-prepared samples.^a

Entry	Catalyst	Conversion (mol%)	H ₂ O ₂ utilization efficiency (%)	Selectivity (mol%) ^b			
				BZA ^c	PHA ^c	SO ^c	Others ^d
1	–	–	–	–	–	–	–
2 ^e	CeO₂	36.5	39.2	47.2	25.3	17.2	10.3
3	CFO-A	32.9	58.8	59.6	19.2	15.0	6.2
4	CFO-Ce_{0.1}	47.6	65.8	75.5	8.5	10.2	5.8
5	CFO-Ce_{0.3}	59.4	68.4	88.2	4.5	3.3	4.0
6	CFO-Ce_{0.5}	41.0	57.7	74.0	11.2	11.2	3.6
7 ^f	Ni _{0.5} Zn _{0.5} Fe ₂ O ₄	30.7	–	52.1	–	–	42.0
8 ^g	Mg _{0.4} Fe _{2.6} O ₄	51.8	–	46.4	2.31	4.63	46.7
9 ^h	Au/TiO ₂	41	–	61.0	–	39.0	–

^a Reaction conditions: styrene: 2.0 mL (17.4 mmol), catalyst: 0.06 mmol, styrene/H₂O₂: 2:3, 1,4-dioxane: 10 mL, 70 °C, 9 h.

^b Selectivity = mol of the given product/mole of the converted styrene.

^c BZA = benzaldehyde, PHA = phenylacetaldehyde, SO = styrene oxide.

^d The main products are benzoic acid and phenylacetic acid.

^e CeO₂ was purchased from Sigma-Aldrich; average particle < 20 nm.

^f From Ref. [26]. Reaction conditions: styrene: 10 mmol, catalyst: 0.42 mmol, styrene/H₂O₂: 1:1, acetone: 10 mL, 60 °C, 12 h.

^g From Ref. [29]. Reaction conditions: styrene: 10 mmol, catalyst: 0.46 mmol, styrene/H₂O₂: 1:2, acetone: 10 mL, 50 °C, 24 h.

^h From Ref. [39]. Reaction conditions: styrene: 2.6 mmol, catalyst, 0.006 mmol (based on Au), styrene/TBHP: 1:1, toluene: 10 mL, 70 °C, 15 h.

Table 4

Effect of catalyst amount on styrene oxidation.^a

Amount of catalyst (mg)	Conversion (mol%)	H ₂ O ₂ utilization efficiency (%)	Selectivity (mol%) ^b			
			BZA ^c	PHA ^c	SO ^c	Others ^d
10.0	53.5	67.1	78.6	11.6	7.6	2.2
15.0	59.4	68.4	88.2	4.5	3.3	4.0
20.0	62.0	63.4	82.4	8.2	6.5	2.9

^a Reaction conditions: styrene: 2.0 mL (17.4 mmol), styrene/H₂O₂: 2:3, 1,4-dioxane: 10 mL, 70 °C, 9 h.

^b Selectivity = moles of the given product/mole of the converted styrene.

^c BZA = benzaldehyde, PHA = phenylacetaldehyde, SO = styrene oxide.

^d The main products are benzoic acid and phenylacetic acid.

the solvent with a high dielectric constant favors styrene conversion, while that with low dielectric constant favors formation of benzaldehyde. The obtained styrene conversion in water, with the highest dielectric constant, was much lower than expected, possibly due to insolubility of styrene in water. The contrary case is that much higher styrene conversion was obtained in 1, 4-dioxane, with the lowest dielectric constant. Much more effort is needed to find convincing explanations for this in future work. From consideration of both styrene conversion and benzaldehyde selectivity, 1,4-dioxane was selected as the proper solvent for the following investigations, which obtained the second highest styrene conversion of 59.4% and the highest benzaldehyde selectivity of 88.2%, as well as the highest H₂O₂ utilization efficiency of 68.4% (entry 5).

3.5. Effect of reaction temperature

The influences of reaction temperature on styrene oxidation were evaluated in the range of 50 to 90 °C for 9 h reaction and the results are listed in Table 6. It can be seen that high temperature favors both styrene conversion and benzaldehyde production. As a result, when temperature was raised from 50 to 90 °C, styrene conversion increased from 21.9 to 90.3% and the selectivity for benzaldehyde increased from 67.3 to 91.5%. The highest H₂O₂ utilization efficiency of 75.1% was also obtained at 90 °C. The selectivities for phenylacetaldehyde and styrene oxide showed a tendency to decrease with increased temperature, while total selectivity for other byproducts increased a little. This indicates that more deeply oxidized products formed at higher temperature.

Table 5
Effect of solvent on styrene oxidation.^a

Entry	Solvent	Conversion (mol%)	H ₂ O ₂ utilization efficiency (%)	Selectivity (mol%) ^b			
				BZA ^c	PHA ^c	SO ^c	Others ^d
1	DMF	64.2	68.2	52.8	9.4	12.3	25.5
2	Pyridine	22.7	43.1	78.4	7.6	8.2	5.8
3	CH ₃ CN	43.2	59.0	66.7	11.2	7.6	14.5
4	Toluene	7.3	19.6	83.8	4.1	5.0	7.1
5	1,4-dioxane	59.4	68.4	88.2	4.5	3.3	4.0
6	Acetylacetone	38.1	55.9	75.8	8.5	8.1	7.6
7	tert-Butanol	22.9	43.3	80.4	6.2	7.8	5.6
8	H ₂ O	44.6	64.0	41.3	32.6	22.3	3.8

^a Reaction conditions: styrene: 2.0 mL (17.4 mmol), **CFO-Ce_{0.3}**: 15.0 mg (0.06 mmol), styrene/H₂O₂: 2:3, solvent: 10 mL, 70 °C, 9 h.^b Selectivity = moles of the given product/mole of the converted styrene.^c BZA = benzaldehyde, PHA = phenylacetaldehyde, SO = styrene oxide.^d The main products are benzoic acid and phenylacetic acid.**Table 6**
Effect of reaction temperature on styrene oxidation.^a

Reaction temperature (°C)	Conversion (mol%)	H ₂ O ₂ utilization efficiency (%)	Selectivity (mol%) ^b			
			BZA ^c	PHA ^c	SO ^c	Others ^d
50	21.9	42.2	67.3	13.0	17.9	1.8
60	39.6	56.9	73.7	11.1	12.7	2.5
70	59.4	68.4	88.2	4.5	3.3	4.0
80	72.4	70.7	89.3	2.9	1.9	5.9
90	90.3	75.1	91.5	1.2	–	7.3

^a Reaction conditions: styrene: 2.0 mL (17.4 mmol), **CFO-Ce_{0.3}**: 15.0 mg (0.06 mmol), styrene/H₂O₂: 2:3, 1,4-dioxane: 10 mL, 9 h.^b Selectivity = moles of the given product/mol of the converted styrene.^c BZA = benzaldehyde, PHA = phenylacetaldehyde, SO = styrene oxide.^d The main products are benzoic acid and phenylacetic acid.

3.6. Effect of styrene/H₂O₂ molar ratio

The effects of different styrene/H₂O₂ molar ratios were investigated and the results are shown in Table 7. It can be seen clearly that, with the molar ratio of styrene/H₂O₂ increased, styrene conversion also increased. As a result, when the molar ratio of styrene/H₂O₂ increased from 2:1 to 2:5, styrene conversion increased from 38.4 to 96.4%. As for the products distribution, the benzaldehyde selectivity increased first from 61.0 to 91.5% when the molar ratio of styrene/H₂O₂ increased from 2:1 to 2:3, but then dropped to 70.5% when the molar ratio of styrene/H₂O₂ further increased to 2:5; the selectivity of phenylacetaldehyde and styrene oxide showed a tendency to decrease with the increased molar ratio of styrene/H₂O₂, while total selectivity for other byproducts increased greatly. This indicates that more deeply oxidized products formed when more oxidant was used. Furthermore, the H₂O₂ utilization efficiency decreased with the increased styrene/H₂O₂ molar ratio. Considering conversion of styrene and selectivity for benzaldehyde, 2:3 was selected as the optimum molar ratio of styrene to H₂O₂.

Table 7
Effect of H₂O₂ amount on styrene oxidation.^a

Styrene/H ₂ O ₂ (mol/mol)	Conversion (mol%)	H ₂ O ₂ utilization efficiency (%)	Selectivity (mol%) ^b			
			BZA ^c	PHA ^c	SO ^c	Others ^d
2:1	38.4	83.7	61.0	13.9	22.1	3.0
1:1	76.3	79.2	78.4	6.7	10.7	4.2
2:3	90.3	75.1	91.5	3.2	–	5.3
1:2	94.6	65.4	82.4	2.4	2.0	13.2
2:5	96.4	56.2	70.5	1.0	1.2	27.3

^a Reaction conditions: styrene: 2.0 mL (17.4 mmol), **CFO-Ce_{0.3}**: 15.0 mg (0.06 mmol), 1,4-dioxane: 10.0 mL, 90 °C, 9 h.^b Selectivity = moles of the given product/mole of the converted styrene.^c BZA = benzaldehyde, PHA = phenylacetaldehyde, SO = styrene oxide.^d The main products are benzoic acid and phenylacetic acid.

3.7. Effect of reaction time

The influence of reaction time on styrene oxidation was investigated at 90 °C in the range 1–10 h with styrene:H₂O₂ molar ratio 2:3. As shown in Table 8, when the reaction time was prolonged from 1 to 10 h, styrene conversion increased from 25.0 to 92.2%; the selectivity for benzaldehyde increased first, but then dropped, and the highest value of 91.5% was obtained for 9 h reaction; the selectivity for phenylacetaldehyde and styrene oxide dropped from 17.7 to 2.5% and from 22.8% to zero, respectively, while the selectivity for total byproducts increased from 0.8 to 13.7% due to more deeply oxidized products being formed. According to the proposed pathway for styrene oxidation (Scheme 1) [67,68], the high yield of benzaldehyde is possibly due to further oxidation of styrene oxide formed in the first step. To confirm this, the stability of styrene oxide and phenylacetaldehyde under the reaction conditions was tested by adding equal molar quantities of styrene oxide (entry 8) or phenylacetaldehyde (entry 9) to the converted styrene and equal molar quantities of H₂O₂ to the residual H₂O₂ based on the first hour's reaction results (entry 1) under the same conditions

Table 8
Effect of reaction time on styrene oxidation.^a

Entry	Reaction time (h)	Conversion (mol%)	H ₂ O ₂ utilization efficiency (%)	Selectivity (mol%) ^b			
				BZA ^c	PHA ^c	SO ^c	Others ^d
1	1	25.0	45.5	58.7	17.7	22.8	0.8
2	3	65.7	68.7	62.8	15.1	20.4	1.7
3	5	79.9	72.7	69.1	11.8	15.3	3.8
4	7	83.2	73.5	74.3	9.5	11.9	4.3
5	8	85.6	74.0	78.9	7.4	8.7	5.0
6	9	90.3	75.1	91.5	3.2	–	5.3
7	10	92.2	71.5	83.8	2.5	–	13.7
8 ^e	1	74.8	–	55.3 ^f	19.3 ^f	24.2 ^f	1.2 ^f
9 ^g	1	3.7	–	–	91.3 ^f	–	3.7 ^h

^a Reaction conditions: styrene: 2.0 mL (17.4 mmol), **CFO-Ce_{0.3}**: 15.0 mg (0.06 mmol), styrene/H₂O₂: 2:3, 1,4-dioxane: 10 mL, 90 °C.

^b Selectivity = moles of the given product/mole of the converted styrene.

^c BZA = benzaldehyde, PHA = phenylacetaldehyde, SO = styrene oxide.

^d The main products are benzoic acid and phenylacetic acid.

^e Only styrene oxide was added.

^f Equal to moles of the given substance/mole of the initially added substrate.

^g Only phenylacetaldehyde was added.

^h Phenylacetic acid.

for 1 h reaction. It can be seen that under the reaction conditions, benzaldehyde transformed from styrene oxide (entry 8) was only 3.4% less than that from direct oxidation of styrene (entry 1), while 3.7% of phenylacetaldehyde was deeply oxidized to phenylacetic acid (entry 9). This confirms that most of the benzaldehyde is derived from styrene oxide. The formation of benzaldehyde may also be facilitated by direct oxidative cleavage of the styrene side chain double bonds [23]. In pursuit of high selectivity for the main product, benzaldehyde, 9 h was selected as the optimum reaction time.

3.8. Reuse of the catalyst

After the reaction, the catalyst can be seen being adsorbed on the magnet. The catalyst together with the magnet can be easily separated by simple decantation after a magnetic field is applied to the surface of the tube, and then subjected to a second run under the same conditions. The results are shown in Fig. 3. The selectivity for benzaldehyde changed slightly after five runs, but the conversion of styrene decreased slightly from 90.3 to 86.8%. The decrease in styrene conversion could be attributed mainly to unavoidable loss of the catalyst during the process of collection. The average

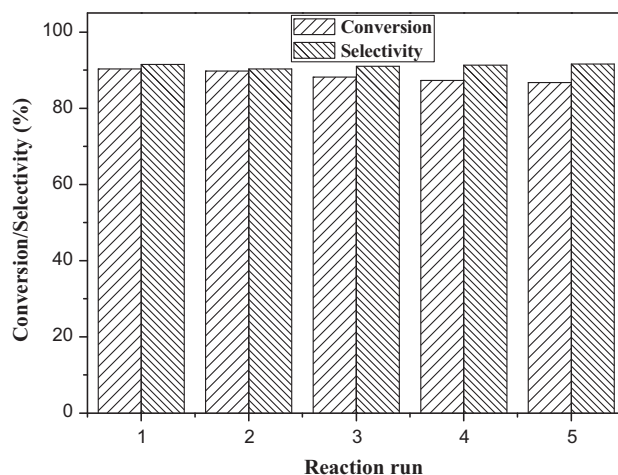


Fig. 3. Reuse of the catalyst **CFO-Ce_{0.3}**. Reaction conditions: styrene: 2.0 mL (17.4 mmol), **CFO-Ce_{0.3}**: 15.0 mg (0.06 mmol), styrene/H₂O₂: 2:3, 1,4-dioxane: 10 mL, 90 °C, 9 h.

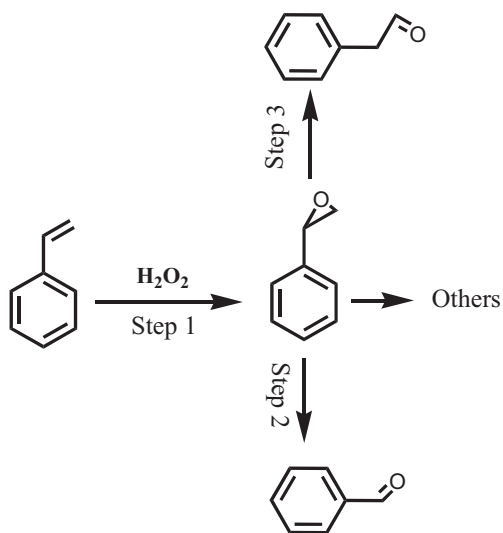
values of styrene conversion and benzaldehyde selectivity were 88.5 and 91.1%, respectively. The results confirm that the sample **CFO-Ce_{0.3}** has good stability and recyclable applicability for the oxidation of styrene under our investigation conditions.

3.9. Extension of substrates

Table 9 shows the results of the investigation of catalysis of oxidation of other olefins by the sample **CFO-Ce_{0.3}** under our optimized conditions. As can be seen, it can effectively catalyze the oxidation of many other cyclic and linear olefins, and above 30% conversion can be obtained. Especially in the case of cyclopentene (entry 1) and α -methylstyrene (entry 3), above 60% conversion and 76% selectivity for the main product were obtained.




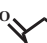

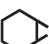
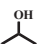
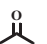


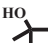


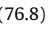
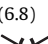
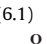

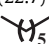
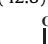
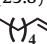




4. Conclusions

Nanosized spinel-type Ce-doped cobalt ferrite complex oxides were prepared by a simple and effective route of sol–gel autocombustion using cheap precursors. The complex ferrite catalysts are more active and easily reusable catalysts for styrene oxidation, and benzaldehyde is the main product. The Ce-doped samples



Scheme 1. Proposed pathway for styrene oxidation.

Table 9
Extension of substrate.^a

Entry	Substrate	Conversion (%) ^b	Selectivity (%) ^b			
1		62.9				Others
2		49.3	(76.7) 	(11.6) 	(4.6) 	(7.1) Others
3		67.9	(2.7) 	(31.5) 	(54.3) 	(11.5) Others
4		39.2	(76.8) 	(6.8) 	(6.1) 	(10.3) Others
5		38.0	(22.7) 	(42.8) 	(23.8) 	(10.7) Others
6		34.1	(32.0) 	(24.2) 	(23.9) 	(19.9) Others
			(19.2)	(39.3)	(35.6)	(5.9)

^a Reaction conditions: catalyst 15.0 mg (0.06 mmol); substrate 2.0 mL; substrate/H₂O₂ ratio 2:3 (mol/mol); 1,4-dioxane: 10 mL; 90 °C, 9 h.

^b Selectivity = moles of the given product/mole of the converted substrate. Entries 1–3 were quantified by GC using toluene as the internal standard, entries 4–6 using decane as the internal standard.

show better performance than pristine CoFe₂O₄ and CeO₂ in enhancement of styrene conversion and benzaldehyde selectivity. The sample Ce_{0.3}Co_{0.7}Fe₂O₄ shows the highest catalytic activity. This work, along with other published ones, indicates that ferrite complex oxides have a considerable potential for becoming a kind of tunable catalysts with respect to catalytic performance and components. Based on this purpose, more efforts have been and will be focused on investigating structure–activity relationships of the ferrite complex oxides in catalytic oxidation reactions.

Acknowledgments

The authors are grateful to the National Natural Science Foundation of China (51302222, 21363021, 21202133), the Natural Science Foundation of Gansu Province (1308RJYA017), and the Program for Changjiang Scholars and Innovative Research Team in University (IRT15R56) for financial support. Siesta DFT calculations in this work were made possible by the facilities of the Shared Hierarchical Academic Research Computing Network (SHARCNET: www.sharcnet.ca) and Compute/Calcul Canada.

Appendix A. Supplementary material

Supplementary data associated with this article can be found, in the online version, at <http://dx.doi.org/10.1016/j.jcat.2016.10.003>.

References

- [1] N. Bahlawane, P.H.T. Ngamou, V. Vannier, T. Kottke, J. Heberle, K. Kohse-Hoinghaus, Tailoring the properties and the reactivity of the spinel cobalt oxide, *Phys. Chem. Chem. Phys.* 11 (2009) 9224–9232.
- [2] J.T. Feng, Y.J. Lin, F. Li, D.G. Evans, D.Q. Li, Preparation, structure and properties of micro-spherical alumina with magnetic spinel ferrite cores, *Appl. Catal. A Gen.* 329 (2007) 112–119.
- [3] G. Baldi, D. Bonacchi, M.C. Franchini, D. Gentili, G. Lorenzi, A. Ricci, C. Ravagli, Synthesis and coating of cobalt ferrite nanoparticles: A first step toward the obtainment of new magnetic nanocarriers, *Langmuir* 23 (2007) 4026–4028.
- [4] T. Bala, C.R. Sankar, M. Baidakova, V. Osipov, T. Enoki, P.A. Joy, B.L.V. Prasad, M. Sastry, Cobalt and magnesium ferrite nanoparticles: Preparation using liquid foams as templates and their magnetic characteristics, *Langmuir* 21 (2005) 10638–10643.
- [5] S. Meng, Z. Yue, L. Li, Effect of ethylene glycol on the orientation and magnetic properties of barium ferrite thin films derived by chemical solution deposition, *J. Magn. Magn. Mater.* 354 (2014) 290–294.
- [6] J. Li, D.L. Dai, X.D. Liu, Y.Q. Lin, Y. Huang, L. Bai, Preparation and characterization of self-formed CoFe₂O₄ ferrofluid, *J. Mater. Res.* 22 (2007) 886–892.
- [7] M.D. Shultz, S. Calvin, P.P. Fatouros, S.A. Morrison, E.E. Carpenter, Enhanced ferrite nanoparticles as MRI contrast agents, *J. Magn. Magn. Mater.* 311 (2007) 464–468.
- [8] B. Peeples, V. Goornavar, C. Peeples, D. Spence, V. Parker, C. Bell, D. Biswal, G.T. Ramesh, A.K. Pradhan, Structural, stability, magnetic, and toxicity studies of nanocrystalline iron oxide and cobalt ferrites for biomedical applications, *J. Nanopart. Res.* 16 (2014) 1–10.
- [9] X.F. Chu, D.L. Jiang, G. Yu, C.M. Zheng, Ethanol gas sensor based on CoFe₂O₄ nano-crystallites prepared by hydrothermal method, *Sens. Actuat. B Chem.* 120 (2006) 177–181.
- [10] Z. Zheng, H. Zhang, Q. Yang, L. Jia, Enhanced high-frequency properties of NiZn ferrite ceramic with Co(2)Z-hexaferrite addition, *J. Am. Ceram. Soc.* 97 (2014) 2016–2019.
- [11] Y. Zhou, G. Yang, Y. Yang, Y. Qin, D. Yin, Y. Zhang, Effect of heating rate on densification and magnetic properties of MnZn ferrites sintered by multiphysical fields coupling methodology, *Adv. Appl. Ceram.* 113 (2014) 257–261.
- [12] A. Meidanchi, O. Akhavan, Superparamagnetic zinc ferrite spinel-graphene nanostructures for fast wastewater purification, *Carbon* 69 (2014) 230–238.
- [13] S. Jovanovic, M. Spreitzer, M. Tramsek, Z. Trontelj, D. Suvorov, Effect of oleic acid concentration on the physicochemical properties of cobalt ferrite nanoparticles, *J. Phys. Chem. C* 118 (2014) 13844–13856.
- [14] A. Yourdkhani, G. Caruntu, Highly ordered transition metal ferrite nanotube arrays synthesized by template-assisted liquid phase deposition, *J. Mater. Chem.* 21 (2011) 7145–7153.
- [15] M. Sheykhan, H. Mohammadnejad, J. Akbari, A. Heydari, Superparamagnetic magnesium ferrite nanoparticles: a magnetically reusable and clean heterogeneous catalyst, *Tetrahedron Lett.* 53 (2012) 2959–2964.
- [16] H. Lee, J.C. Jung, I.K. Song, Oxidative dehydrogenation of n-butene to 1,3-butadiene over sulfated ZnFe₂O₄ catalyst, *Catal. Lett.* 133 (2009) 321–327.
- [17] Y.M. Chung, Y.T. Kwon, T.J. Kim, S.J. Lee, S.H. Oh, Prevention of catalyst deactivation in the oxidative dehydrogenation of n-butene to 1,3-butadiene over Zn-ferrite catalysts, *Catal. Lett.* 131 (2009) 579–586.
- [18] J. Tasca, A. Lavat, K. Nesprias, G. Barreto, E. Alvarez, N. Eyler, A. Canizo, Cyclic organic peroxides thermal decomposition in the presence of CuFe₂O₄ magnetic nanoparticles, *J. Mol. Catal. A Chem.* 363 (2012) 166–170.

- [19] D. Fino, N. Russo, G. Saracco, V. Specchia, CNG engines exhaust gas treatment via Pd-spinel-type-oxide catalysts, *Catal. Today* 117 (2006) 559–563.
- [20] E. Casbeer, V.K. Sharma, X.-Z. Li, Synthesis and photocatalytic activity of ferrites under visible light: a review, *Sep. Purif. Technol.* 87 (2012) 1–14.
- [21] Q.S. Liu, J.F. Yu, P.P. Yang, Z.L. Wang, X.W. Yang, T.H. Wu, Influence of cation distribution of ZnFe_2O_4 on its catalytic activity of phenol hydroxylation with H_2O_2 , *Chem. J. Chin. Univ. Chin.* 25 (2004) 701–704.
- [22] R. Klimkiewicz, H. Grabowska, W. Mista, K. Przybylski, Mg-Zn and Mn-Zn ferrites derived from coil core materials as new phenol methylation catalysts, *Ind. Eng. Chem. Res.* 51 (2012) 2205–2213.
- [23] B. Jager, A. Wermann, P. Scholz, M. Müller, U. Reislohner, A. Stolle, B. Ondruschka, Iron-containing defect-rich mixed metal oxides for Friedel-Crafts alkylation, *Appl. Catal. A Gen.* 443 (2012) 87–95.
- [24] Q. Yang, J. Liu, L. Zhang, C. Li, Functionalized periodic mesoporous organosilicas for catalysis, *J. Mater. Chem.* 19 (2009) 1945–1955.
- [25] F. Papa, L. Patron, O. Carp, C. Paraschiv, B. Ioan, Catalytic activity of neodymium substituted zinc ferrites for oxidative conversion of methane, *J. Mol. Catal. A Chem.* 299 (2009) 93–97.
- [26] D. Guin, B. Baruwati, S.V. Manorama, A simple chemical synthesis of nanocrystalline AFe_2O_4 (A = Fe, Ni, Zn): an efficient catalyst for selective oxidation of styrene, *J. Mol. Catal. A Chem.* 242 (2005) 26–31.
- [27] G. Evans, I.V. Kozhevnikov, E.F. Kozhevnikova, J.B. Claridge, R. Vaidhyanathan, C. Dickinson, C.D. Wood, A.I. Cooper, M.J. Rosseinsky, Particle size-activity relationship for CoFe_2O_4 nanoparticle CO oxidation catalysts, *J. Mater. Chem.* 18 (2008) 5518–5523.
- [28] S.K. Pardeshi, R.Y. Pawar, SrFe_2O_4 complex oxide an effective and environmentally benign catalyst for selective oxidation of styrene, *J. Mol. Catal. A Chem.* 334 (2011) 35–43.
- [29] N. Ma, Y.H. Yue, W.M. Hua, Z. Gao, Selective oxidation of styrene over nanosized spinel-type $\text{Mg}_x\text{Fe}_{3-x}\text{O}_4$ complex oxide catalysts, *Appl. Catal. A Gen.* 251 (2003) 39–47.
- [30] X. Zhao, W. Wang, Y. Zhang, S. Wu, F. Li, J.P. Liu, Synthesis and characterization of gadolinium doped cobalt ferrite nanoparticles with enhanced adsorption capability for Congo Red, *Chem. Eng. J.* 250 (2014) 164–174.
- [31] Y.J. Yang, M.M. Yang, Z.L. Luo, C.S. Hu, J. Bao, H.L. Huang, S. Zhang, J.W. Wang, P. S. Li, Y. Liu, Y.G. Zhao, X.C. Chen, G.Q. Pan, T. Jiang, Y.K. Liu, X.G. Li, C. Gao, Anomalous thickness-dependent strain states and strain-tunable magnetization in Zn-doped ferrite epitaxial films, *J. Appl. Phys.* 115 (2014) E304–E311.
- [32] B. Xiao, S.-Q. Liu, Enhancing the photocatalytic activity of nickel ferrite doped with graphene, *Asian J. Chem.* 26 (2014) 1391–1393.
- [33] M. Srivastava, S. Layek, J. Singh, A.K. Das, H.C. Verma, A.K. Ojha, N.H. Kim, J.H. Lee, Synthesis, magnetic and Mossbauer spectroscopic studies of Cr doped lithium ferrite nanoparticles, *J. Alloys Compd.* 591 (2014) 174–180.
- [34] I. Sabikoglu, L. Parali, FT-IR and VSM properties of samarium-doped nickel ferrite, *Funct. Mater. Lett.* 7 (2014) 1450046–1–5.
- [35] P. Samoilă, T. Slatineanu, P. Postolache, A.R. Iordan, M.N. Palamaru, The effect of chelating/combustion agent on catalytic activity and magnetic properties of Dy doped Ni-Zn ferrite, *Mater. Chem. Phys.* 136 (2012) 241–246.
- [36] A.V. Raut, R.S. Barkule, D.R. Shengule, K.M. Jadhav, Synthesis, structural investigation and magnetic properties of Zn^{2+} substituted cobalt ferrite nanoparticles prepared by the sol-gel auto-combustion technique, *J. Magn. Magn. Mater.* 358 (2014) 87–92.
- [37] C. Cannas, A. Musinu, D. Peddis, G. Piccaluga, New synthesis of ferrite-silica nanocomposites by a sol-gel auto-combustion, *J. Nanopart. Res.* 6 (2004) 223–232.
- [38] A. Dhakshinamoorthy, M. Alvaro, H. Garcia, Aerobic oxidation of styrenes catalyzed by an iron metal organic framework, *ACS Catal.* 1 (2011) 836–840.
- [39] M. Nemanashi, R. Meijboom, Dendrimer derived titania-supported Au nanoparticles as potential catalysts in styrene oxidation, *Catal. Lett.* 143 (2013) 324–332.
- [40] Q.H. Yang, C. Li, S.D. Yuan, J. Li, P.L. Ying, Q. Xin, W.D. Shi, Epoxidation of styrene on a novel titanium-silica catalyst prepared by ion beam implantation, *J. Catal.* 183 (1999) 128–130.
- [41] J.M. Mitchell, N.S. Finney, New molybdenum catalysts for alkyl olefin epoxidation. Their implications for the mechanism of oxygen atom transfer, *J. Am. Chem. Soc.* 123 (2001) 862–869.
- [42] F.E. Kuhn, M. Groarke, E. Bencze, E. Herdtweck, A. Prazeres, A.M. Santos, M.J. Calhorda, C.C. Romão, I.S. Goncalves, A.D. Lopes, M. Pillinger, Octahedral bipyridine and bipyrimidine dioxomolybdenum(VI) complexes: Characterization, application in catalytic epoxidation, and density functional mechanistic study, *Chem. Eur. J.* 8 (2002) 2370–2383.
- [43] N.T. Thao, N.D. Trung, D.V. Long, Activity of molybdate-intercalated layered double hydroxides in the oxidation of styrene with air, *Catal. Lett.* 146 (2016) 918–928.
- [44] N.T. Thao, H.H. Trung, Selective oxidation of styrene over Mg-Co-Al hydrotalcite like-catalysts using air as oxidant, *Catal. Commun.* 45 (2014) 153–157.
- [45] Y.H. Fu, L. Xu, H.M. Shen, H. Yang, F.M. Zhang, W.D. Zhu, M.H. Fan, Tunable catalytic properties of multi-metal-organic frameworks for aerobic styrene oxidation, *Chem. Eng. J.* 299 (2016) 135–141.
- [46] L. Wang, B.S. Zhang, W. Zhang, J. Zhang, X.H. Gao, X.J. Meng, D.S. Su, F.S. Xiao, Positively charged bulk Au particles as an efficient catalyst for oxidation of styrene with molecular oxygen, *Chem. Commun.* 49 (2013) 3449–3451.
- [47] A.S. Sharma, D. Shah, H. Kaur, Gold nanoparticles supported on dendrimer@resin for the efficient oxidation of styrene using elemental oxygen, *RSC Adv.* 5 (2015) 42935–42941.
- [48] A. Dhakshinamoorthy, M. Latorre-Sanchez, A.M. Asiri, A. Primo, H. Garcia, Sulphur-doped graphene as metal-free carbocatalysts for the solventless aerobic oxidation of styrenes, *Catal. Commun.* 65 (2015) 10–13.
- [49] M.J. Rak, M. Lerro, A. Moores, Hollow iron oxide nanoshells are active and selective catalysts for the partial oxidation of styrene with molecular oxygen, *Chem. Commun.* 50 (2014) 12482–12485.
- [50] S. Urus, H. Achguzel, M. Incesu, Synthesis of novel N_4O_4 type bis(diazoimine)-metal complexes supported on mesoporous silica: Microwave assisted catalytic oxidation of cyclohexane, cyclooctane, cyclohexene and styrene, *Chem. Eng. J.* 296 (2016) 90–101.
- [51] M. Farrag, Monodisperse and polydisperse platinum nanoclusters supported over TiO_2 anatase as catalysts for catalytic oxidation of styrene, *J. Mol. Catal. A Chem.* 413 (2016) 67–76.
- [52] B. Wang, J. Zhang, X. Zou, H.G. Dong, P.J. Yao, Selective oxidation of styrene to 1,2-epoxyethylbenzene by hydrogen peroxide over heterogeneous phosphomolybdic acid supported on ionic liquid modified MCM-41, *Chem. Eng. J.* 260 (2015) 172–177.
- [53] Y. Wan, Q. Liang, Z. Li, S. Xu, X. Hu, Q. Liu, D. Lu, Significant improvement of styrene oxidation over zinc phthalocyanine supported on multi-walled carbon nanotubes, *J. Mol. Catal. A Chem.* 402 (2015) 29–36.
- [54] S. Ghosh, S.S. Acharyya, M. Kumar, R. Bal, One-pot preparation of nanocrystalline Ag-WO_3 catalyst for the selective oxidation of styrene, *RSC Adv.* 5 (2015) 37610–37616.
- [55] H. Wang, W. Qian, J. Chen, Y. Wu, X. Xu, J. Wang, Y. Kong, Spherical V-MCM-48: the synthesis, characterization and catalytic performance in styrene oxidation, *RSC Adv.* 4 (2014) 50832–50839.
- [56] J. Wang, J. Lu, J. Yang, R. Chen, Y. Zhang, D. Yin, J. Wang, Ti containing mesoporous silica submicrometer-sphere, with tunable particle size for styrene oxidation, *Appl. Surf. Sci.* 283 (2013) 794–801.
- [57] F. Rajabi, N. Karimi, M.R. Saidi, A. Primo, R.S. Varma, R. Luque, Unprecedented selective oxidation of styrene derivatives using a supported iron oxide nanocatalyst in aqueous medium, *Adv. Synth. Catal.* 354 (2012) 1707–1711.
- [58] S.K. Pardeshi, R.Y. Pawar, Optimization of reaction conditions in selective oxidation of styrene over fine crystallite spinel-type CaFe_2O_4 complex oxide catalyst, *Mater. Res. Bull.* 45 (2010) 609–615.
- [59] R. Ramanathan, S. Sugunan, Styrene oxidation by H_2O_2 using Ni-Gd ferrites prepared by co-precipitation method, *Catal. Commun.* 8 (2007) 1521–1526.
- [60] X.D. Cai, H.Y. Wang, Q.P. Zhang, J.H. Tong, Selective oxidation of styrene efficiently catalyzed by spinel Mg-Cu ferrite complex oxides in water, *J. Sol-Gel Sci. Technol.* 69 (2014) 33–39.
- [61] D.-H. Zhang, H.-B. Li, G.-D. Li, J.-S. Chen, Magnetically recyclable Ag-ferrite catalysts: general synthesis and support effects in the epoxidation of styrene, *Dalton Trans.* 10527–10533 (2009).
- [62] J.H. Tong, L.L. Bo, Z. Li, Z.Q. Lei, C.G. Xia, Magnetic CoFe_2O_4 nanocrystal: a novel and efficient heterogeneous catalyst for aerobic oxidation of cyclohexane, *J. Mol. Catal. A Chem.* 307 (2009) 58–63.
- [63] L.P. Zhou, J. Xu, H. Miao, F. Wang, X.Q. Li, Catalytic oxidation of cyclohexane to cyclohexanol and cyclohexanone over Co_3O_4 nanocrystals with molecular oxygen, *Appl. Catal. A Gen.* 292 (2005) 223–228.
- [64] C. Chen, J. Xu, Q.H. Zhang, H. Ma, H. Miao, L.P. Zhou, Direct synthesis of bifunctionalized hexagonal mesoporous silicas and its catalytic performance for aerobic oxidation of cyclohexane, *J. Phys. Chem. C* 113 (2009) 2855–2860.
- [65] F. Chen, X. Shen, Y. Wang, J. Zhang, $\text{CeO}_2/\text{H}_2\text{O}_2$ system catalytic oxidation mechanism study via a kinetics investigation to the degradation of acid orange 7, *Appl. Catal. B Environ.* 121 (2012) 223–229.
- [66] J.M. Soler, E. Artacho, J.D. Gale, A. García, J. Junquera, P. Ordejón, D. Sánchez-Portal, The SIESTA method for ab initio order-N materials simulation, *J. Phys. Condens. Matter* 14 (2002) 2745–2779.
- [67] M.R. Maurya, A.K. Chandrakar, S. Chand, Oxidation of phenol, styrene and methyl phenyl sulfide with H_2O_2 catalysed by dioxovanadium(V) and copper (II) complexes of 2-aminomethylbenzimidazole-based ligand encapsulated in zeolite-Y, *J. Mol. Catal. A Chem.* 263 (2007) 227–237.
- [68] G. Romanowski, J. Kira, Oxidovanadium(V) complexes with chiral tridentate Schiff bases derived from R(-)-phenylglycinol: synthesis, spectroscopic characterization and catalytic activity in the oxidation of sulfides and styrene, *Polyhedron* 53 (2013) 172–178.